General Disclaimer

One or more of the Following Statements may affect this Document

- This document has been reproduced from the best copy furnished by the organizational source. It is being released in the interest of making available as much information as possible.

- This document may contain data, which exceeds the sheet parameters. It was furnished in this condition by the organizational source and is the best copy available.

- This document may contain tone-on-tone or color graphs, charts and/or pictures, which have been reproduced in black and white.

- This document is paginated as submitted by the original source.

- Portions of this document are not fully legible due to the historical nature of some of the material. However, it is the best reproduction available from the original submission.

OLD DOMINION UNIVERSITY RESEARCH FOUNDATION

DEPARTMENT OF MECHANICAL ENGINEERING AND MECHANICS
SCHOOL OF ENGINEERING
OLD DOMINION UNIVERSITY
NORFOLK, VIRGINIA 23508

INVESTIGATION OF CHEMICALLY-REACTING SUPERSONIC INTERNAL FLOWS

By

T. Chitsomboon, Graduate Research Assistant

and

S. N. Tiwari, Principal Investigator

Progress Report
For the period ending July 31, 1985

Prepared for the
National Aeronautics and Space Administration
Langley Research Center
Hampton, Virginia 23665

Under
Research Grant NAG-1-423
Dr. Ajay Kumar, Technical Monitor
HSAD-Computational Methods Branch

September 1985

DEPARTMENT OF MECHANICAL ENGINEERING AND MECHANICS
SCHOOL OF ENGINEERING
OLD DOMINION UNIVERSITY
NORFOLK, VIRGINIA 23508

INVESTIGATION OF CHEMICALLY-REACTING SUPERSONIC INTERNAL FLOWS

By

T. Chitsomboon, Graduate Research Assistant

and

S. N. Tiwari, Principal Investigator

Progress Report
For the period ending July 31, 1985

Prepared for the
National Aeronautics and Space Administration
Langley Research Center
Hampton, Virginia 23665

Under
Research Grant NAG-1-423
Dr. Ajay Kumar, Technical Monitor
HSAD-Computational Methods Branch

Submitted by the
Old Dominion University Research Foundation
P. O. Box 6369
Norfolk, Virginia 23508

September 1985

FOREWORD

This report covers the work completed on the research project "Analysis and Computation of Internal Flow Field in a Scramjet Engine" for the period ending July 31, 1985. The work was supported by the NASA Langley Research Center (Computational Methods Branch of the High-Speed Aerodynamics Division) through research grant NAG-1-423; the grant was monitored by Dr. Ajay Kumar of the High-Speed Aerodynamics Branch.

ABSTRACT

The governing equations of two-dimensional chemically-reacting flows are presented together with the global two-step chemistry model. The finite-difference algorithm used is illustrated and the method of circumventing the stiffness is discussed. The computer program developed is used to solve two model problems of a premixed chemically-reacting flow. The results obtained are physically reasonable.

LIST OF SYMBOLS

a_i, b_i	constants for evaluating the specific heat of the ith species
$\bar{C}_p$	mixture specific heat at constant pressure
$\bar{C}_v$	mixture specific heat at constant volume
D	diffusion coefficient
e_t	total specific energy
f_i	mass fraction of the ith species
h	enthalpy
H	total specific enthalpy of the mixture
H_i°	enthalpy of formation at 0° K of the ith species
J	Jacobian of coordinates transformation
k_{bi}, k_{fi}	backward, forward reaction rate coefficients for the ith reaction eq.
Le	Lewis number
M_i	molecular weight of the ith species
p	pressure
Pr_ℓ	laminar Prandtl number
Pr_t	turbulent Prandtl number
q	dependent variable vector
R_i	gas constant of the ith species
$\bar{R}$	mixture gas constant
T	temperature
u, v	velocity in the x, y directions
α	thermal diffusivity
ξ, η	computational coordinates
μ_ℓ, μ_t	laminar, turbulent viscosities

ν	kinamatic viscosity
ρ	mixture density
ρ_i	density of the ith species

TABLE OF CONTENTS

LIST OF TABLES

LIST OF FIGURES

TABLE OF CONTENTS - Continued

LIST OF FIGURES

INVESTIGATION OF CHEMICALLY-REACTING SUPERSONIC INTERNAL FLOWS

By

T. Chitsomboon[1] and S. N. Tiwari[2]

1. INTRODUCTION

The NASA Langley Research Center has been involved in research to develop a supersonic combustion ramjet (scramject) propulsion system for a number of years (Refs. 1-3). Numerical calculations of the flow fields in various regions of scramjet engines have proved to be valuable in understanding the nature of these flows. The flows of pure air through the scramjet engines were studied numerically by Kumar (Refs. 4-6). Drummond and Weidner (Ref. 7) assumed a complete-reaction model to study the effect of gaseous hydrogen fuel injection from the side walls and from the center strut. The complete-reaction model, however, could predict the extent of combustion by orders of magnitude higher than that of the actual combustion. A realistic combustion model of the hydrogen-air system would involve some 60 reaction paths (Ref. 8) which would make numerical investigations very costly if not impossible. The global two-step combustion model (Ref. 9) offers an alternative between these two extremes. In this global model, only two reaction paths and four species of reactant and oxidizer are involved. Use of this reaction model should make numerical study of the H_2-air reacting system feasible while maintaining important features of the real combustion phenomena such as the extent of mixing and the overall heat release.

---

[1]Graduate Research Assistant, Department of Mechanical Engineering and Mechanics, Old Dominion University, Norfolk, Virginia 23508.
[2]Eminent Professor, Department of Mechanical Engineering and Mechanics, Old Dominion University, Norfolk, Virginia 23508.

The system of equations governing the H_2-air reacting flow is stiff due to the fast reaction associated with the global two-step chemistry model. Numerical integration of these equations by means of explicit time-dependent finite difference methods requires extremely small time steps to ensure stability. The stable time-step magnitudes are usually orders of magnitude smaller than the time steps dictated by the CFL number of the fluid-dynamics equations. The small time steps that have to be used impose a severe restriction on computer resources. One way of getting around the stiff criterion is by integrating all the governing equations by fully-implicit methods. The system of algebraic equations resulting from fully-implicit methods usually requires large computer storage in addition to complicated algorithm and long matrix-inversion time. With the advent of vector computers, such as the VPS-32 at the NASA Langley Research Center, an explicit method might be more attractive because it is fully vectorizable. With the above mentioned stiffness, however, a fully-vectorized code could still result in a very long integration time before a steady state is reached.

Another approach in integrating the stiff equations is by evaluating the terms that give rise to stiffness implicitly while the other terms, not contributing to stiffness, are evaluated explicitly (Refs. 10 and 11). This technique allows integration of the fluid-dynamic equations by an explicit method using the fluid-dynamics time steps calculated from the CFL condition. The species equations, however, produce a block-diagonal system of algebraic equations since the source terms (the terms that give rise to the stiffness) are evaluated implicitly. The block-diagonal system can be inverted relatively economically as compared to inversion of a multi-diagonal system resulting from a fully-implicit method. Also, a large portion of the code is still vectorizable which makes this approach

particularly efficient on a vector computer. Drummond et al. (Ref. 12) successfully used this technique, with the global two-step reaction model, in combination with a spectral method to solve a quasi-one-dimensional reacting internal flow of premixed H_2-air system. Bussing and Murman (Ref. 13) independently used the same procedure to calculate inviscid premixed H_2-air reacting system by a finite-volume method.

The purpose of this investigation is to develop a computer code to calculate a realistic chemically-reacting flow field in a scramjet engine by using the two-dimensional Navier-Stokes equations and species equations together with the global two-step reaction model of Ref. 8. The two-dimensional full Navier-Stokes solver of Kumar (Ref. 14-15) will be modified to incorporate the chemistry package. Turbulence is modeled according to the two-layer eddy viscosity model of Ref. 16.

2. ANALYSIS

The governing equations of the H_2-air reacting system is presented in Section 2.1. Section 2.2 briefly discussed the chemistry model used in this study. The thermodynamics model is discussed in Section 2.3.

2.1 Governing Equations

The two-dimensional Navier-Stokes equations in body-fitted coordinates written in the strong conservation-law form can be expressed symbolically as

$$\frac{\partial q}{\partial t} + \frac{\partial E}{\partial \xi} + \frac{\partial F}{\partial \eta} = 0 \qquad (2.1)$$

where

$$q \equiv J \begin{bmatrix} \rho \\ \rho u \\ \rho v \\ \rho H - p \end{bmatrix}$$

$$E \equiv \begin{bmatrix} \rho\bar{u} \\ \rho u\bar{u} + y_\eta \tau_{xx} - x_\eta \tau_{xy} \\ \rho v\bar{u} + y_\eta \tau_{yx} - x_\eta \tau_{yy} \\ (\rho H - p)\bar{u} + y_\eta (u\tau_{xx} + v\tau_{xy} + q_x) - x_\eta (v\tau_{yy} + u\tau_{yx} + q_y) \end{bmatrix}$$

$$F \equiv \begin{bmatrix} \rho\bar{v} \\ \rho u\bar{v} - y_\xi \tau_{xx} + x_\xi \tau_{xy} \\ \rho v\bar{v} - y_\xi \tau_{yx} + x_\xi \tau_{yy} \\ (\rho H - p)\bar{v} - y_\xi (u\tau_{xx} + v\tau_{xy} + q_x) + x_\xi (u\tau_{yx} + v\tau_{yy} + q_y) \end{bmatrix}$$

Here, x_ξ denotes $\partial x/\partial \xi$, and so forth, and

$$\bar{u} = y_\eta u - x_\eta v \tag{2.2a}$$

$$\bar{v} = -y_\xi u + x_\xi v \tag{2.2b}$$

$$J = x_\xi y_\eta - x_\eta y_\xi \tag{2.2c}$$

The quantities τ_{xx}, τ_{xy}, τ_{yx} and τ_{yy} are components of the stress tensor and are given by (with the Stokes' hypothesis assumed)

$$\tau_{xx} = p - \frac{4}{3}\mu\frac{\partial u}{\partial x} + \frac{2}{3}\mu\frac{\partial v}{\partial y} \tag{2.3a}$$

$$\tau_{xy} = \tau_{yx} = -\mu\left(\frac{\partial u}{\partial y} + \frac{\partial v}{\partial x}\right) \tag{2.3b}$$

$$\tau_{yy} = p + \frac{2}{3}\mu\frac{\partial u}{\partial x} - \frac{4}{3}\mu\frac{\partial v}{\partial y} \tag{2.3c}$$

The quantities q_x and q_y are components of the heat flux and are given by

$$q_x = -\left(\frac{\mu_\ell}{Pr_\ell} + \frac{\mu_t}{Pr_t}\right)\frac{\partial h}{\partial x} \tag{2.4a}$$

$$q_y = -\left(\frac{\mu_\ell}{Pr_\ell} + \frac{\mu_t}{Pr_t}\right)\frac{\partial h}{\partial y} \tag{2.4b}$$

By assuming a thermally perfect gas, H and h can be given as

$$H = \sum_{i=1}^{5} f_i H_i^\circ + \bar{C}_p T + .5\,(u^2+v^2) \tag{2.5}$$

$$h = \bar{C}_p T \tag{2.6}$$

The μ_ℓ is determined by the Sutherland's formula whereas the μ_t is calculated by using the two-layer eddy viscosity model of Ref. 16. Pure air properties are used to calculate μ_ℓ and μ_t since the combustion products are dominated by the nitrogen species. Finally, to close the system of equations the ideal gas equation of state, $p = \rho\bar{R}T$, is used. The gas constant, $\bar{R}$, is calculated by averaging over the mixture.

The global two-step reaction model used in this study contains five chemical species, i.e., O_2, H_2O, H_2, OH and N_2; they will be referred to in the following discussion by the subscripts 1, 2, 3, 4 and 5, respectively.

The strong conservation-law form of the two-dimensional species continuity equations can be written in body-fitted coordinates as

$$\frac{\partial q_i}{\partial t} + \frac{\partial E_i}{\partial \xi} + \frac{\partial F_i}{\partial \eta} = JW_i; \quad i = 1,2,3,4 \tag{2.7}$$

where

$$q_i = J\rho f_i = J\rho_i \tag{2.8a}$$

$$E_i = \rho_i \bar{u} - y_\eta\left(\beta \frac{\partial f_i}{\partial x}\right) + x_\eta \left(\beta \frac{\partial f_i}{\partial y}\right) \tag{2.8b}$$

$$F_i = \rho_i \bar{v} + y_\xi\left(\beta \frac{\partial f_i}{\partial x}\right) - x_\xi \left(\beta \frac{\partial f_i}{\partial y}\right) \tag{2.8c}$$

The quantities $\bar{u}$ and $\bar{v}$ are as defined in the previous discussion. The quantity β is defined as

$$\beta = \frac{\mu}{Le \cdot Pr} \tag{2.9}$$

where

$$Le = \alpha/D \tag{2.10}$$

and

$$Pr = \nu/\alpha \tag{2.11}$$

In this study the Lewis number (Le) is assumed to be equal to 1. This assumption is reasonable for the gaseous mixture of the present study. The assumption also provides a great simplification of the governing equations. In particular, the enthalpy transported by species diffusions can be combined with the heat diffusion terms to yield the terms q_x and q_y as indicated in Eq. (2.4). A detailed discussion can be found in Ref. 17. Moreover, there is no need to evaluate the species diffusion coefficient D.

Note that only four species equations are actually solved. The nitrogen species is assumed to be inert. The mass fraction of nitrogen can be evaluated by the following relation:

$$f_5 = 1 - \sum_{i=1}^{4} f_i \tag{2.12}$$

The above relation is nothing but the mass conservation law of the mixture.

2.2 Chemistry Model

The global two-step reaction model is given by

$$H_2 + O_2 \underset{k_{b1}}{\overset{k_{f1}}{\rightleftharpoons}} 2\,OH \qquad (2.13a)$$

$$2\,OH + H_2 \underset{k_{b2}}{\overset{k_{f2}}{\rightleftharpoons}} 2\,H_2O \qquad (2.13b)$$

where the k_f's are the forward reaction rate constants and the k_b's are the backward reaction rate constants. The numerical values of k_f's and k_b's as well as the details of this chemistry model are given in Ref. 9.

For a general reaction

$$\sum_{j=1}^{N} Z_{ij}\, C_j \underset{k_{bi}}{\overset{k_{fi}}{\rightleftharpoons}} \sum_{j=1}^{N} \hat{Z}_{ij}\, C_j, \quad i=1,2\ldots,I$$

the rate of production (or extinction) of species j, can be obtained from the law of mass action as

$$(C_j')_i = (\hat{Z}_{ij} - Z_{ij})\left(k_{fi} \prod_{j=1}^{N} C_j^{Z_{ij}} - k_{bi} \prod_{j=1}^{N} C_j^{\hat{Z}_{ij}}\right) \qquad (2.14)$$

The rate of change of the molar concentration of species j is found by summing over all the reaction equations, i.e.,

$$C_j' = \sum_{i=1}^{I} (C_j')_i \qquad (2.15)$$

The rate of change of mass concentration of species j is found from

$$W_j = C'_j M_j \tag{2.16}$$

By applying the procedure of Eqs. (2.14) through (2.16) to Eq. (2.13), the following mass production rates are obtained:

$$W_1 = -\frac{k_{f1}\rho_1\rho_3}{M_3} + \frac{k_{b1}M_1\rho_4^2}{2M_4} \tag{2.17a}$$

$$W_2 = \frac{2k_{f2}M_2\rho_3\rho_4^2}{2M_3M_4} - \frac{2k_{b2}\rho_2^2}{M_2} \tag{2.17b}$$

$$W_3 = \frac{M_3W_1}{M_1} - \frac{M_3W_2}{2M_2} \tag{2.17c}$$

$$W_4 = -\frac{2M_4W_1}{M_1} - \frac{M_4W_2}{M_2} \tag{2.17d}$$

The W_i terms above are used in the right-hand side of Eq. 2.7.

2.3 Thermodynamics Model

The value of the specific heat at constant pressure, C_p, is assumed to be a linear function of temperature. The arbitrary constants are obtained from curve fitting the temperature data of Ref. 18. For each species, the specific heat is, therefore, expressed as

$$C_{pi} = a_iT + b_i \tag{2.18}$$

The total enthalpy of the mixture is given by

$$H = \sum_{i=1}^{5} \left[f_i \int_{\circ}^{T} (C_{pi}\, dT + H_i^{\circ}) \right] + \frac{1}{2}(u^2 + v^2) \qquad (2.19)$$

Using Eq. (2.18) in Eq. (2.19) and integrating gives

$$H = \sum_{i=1}^{5} \left[f_i (0.5 a_i T^2 + b_i T + H_i^{\circ}) \right] + \frac{1}{2}(u^2 + v^2) \qquad (2.20)$$

The mixture gas constant can be obtained by summation over all species as

$$\bar{R} = \sum_{i=1}^{5} f_i R_i \qquad (2.21)$$

The numerical values of various thermodynamic constants are summarized in Table 1 below.

Table 1. Numerical values of various thermodynamic constants.

Species	H_i° (Joule/kg)	a	b	R_i (Joule/kg.K)
O_2	-271,267	0.1198	947	254
H_2O	-13,972,530	0.4391	1858	457
H_2	-4,200,188	2.0546	12867	4035
OH	+1,772,591	0.1656	1673	478
N_2	-309,483	0.1035	1048	240

The values in Table 1 above are obtained from Ref. 19.

3. FINITE DIFFERENCE ALGORITHM

The Eqs. (2.1) and (2.7) can be differenced in time as (for simplicity, the subscript i has been dropped in the subsequent discussion)

$$q^{n+1} - q^n = -\Delta t \left(\frac{\partial E^n}{\partial \xi} + \frac{\partial F^n}{\partial \eta} - JW^{n+1}\right) + 0\,(\Delta t)^2 \qquad (3.1)$$

where (n+1) denotes the time level where solutions are being sought. It is to be understood that the source terms, W's, are equal to zero for the fluid-dynamics equations. Note that the source terms are evaluated at the implicit time level (n+1) to alleviate stiffness associated with fast chemical reactions as discussed earlier. Before developing a discrete form of the Eq. (3.1) the nonlinear implicit quantities must be linearized in order to render a linear discrete equation for solution. Using Newtonian linearization one obtains

$$W^{n+1} = W^n + \left(\frac{\partial W^n}{\partial q}\right)\left(q^{n+1} - q^n\right) \qquad (3.2)$$

The q's in the above equation are the $J\rho_i$'s of the four species. Since both W and q are vectors of four elements, the term $\partial w/\partial q$ becomes a 4x4 matrix, the Jacobian matrix.

Upon defining

$$A \equiv J \frac{\partial w}{\partial q}$$

$$\Delta q^n \equiv q^{n+1} - q^n$$

$$R^n \equiv \frac{\partial E^n}{\partial \xi} + \frac{\partial F^n}{\partial \eta} - JW^n$$

and substituting Eq. (3.2) into Eq. (3.1) and rearranging one obtains

$$(I - \Delta t A)^n \Delta q^n = - \Delta t \, (R^n) \qquad (3.3)$$

where I is the 8x8 identity matrix.

A discrete form of Eq. (3.3) can be advanced in time using the explicit unsplit MacCormack algorithm (Ref. 20) as follows

Predictor Step:

$$(I - \Delta t A)^n \overline{\Delta q^n} = - \Delta t \, R_f^n \qquad (3.4)$$

$$\overline{q^{n+1}} = q^n + \overline{\Delta q^n} \qquad (3.5)$$

Corrector Step:

$$(I - \Delta t A)^{\overline{n+1}} \Delta q^n = - \Delta t R_b^{\overline{n+1}} \qquad (3.6)$$

$$q^{n+1} = q^n + \frac{1}{2} (\overline{\Delta q^n} + \Delta q^n) \qquad (3.7)$$

The subscript f and b in Eqs. (3.4) and (3.6) denote forward and backward finite differences, respectively. In this study, only the steady-state solution is sought. The time step (Δt) used is determined from the

CFL condition:

$$\Delta t = \min \left(\frac{\Delta x}{|u| + a} , \frac{\Delta y}{|v| + a} \right) \qquad (3.8)$$

If accurate temporal history is desired one has to choose Δt in a different manner (see, e.g., Ref. 12).

The boundary conditions used in this study are the no-slip conditions, the adiabatic wall condition, the zero normal pressure gradient condition and the non-catalytic conditions. The non-catalytic conditions assume zero normal concentration gradients for all species. At the inflow boundary, all dependent variables are fixed according to the free stream conditions of interest. The method of extrapolation is used at the outflow boundary, this limits the application to supersonic outflow only. For a subsonic outflow, an appropriate method must be employed.

Numerical smoothing functions are also added to the algorithm for both the fluid-dynamics and the species equations. The functions used for the fluid equation can be found in Refs. 4-6. For the species equations, the same form of the smoothing functions used in the fluid equations are employed; only the dependent variables are changed. The addition of the smoothing functions to the species equations was found to be necessary in order to suppress high frequency oscillations in species densities.

4. SOLUTION PROCEDURE

The fluid-dynamics part of the flow is integrated in time from an initial solution by the fully explicit MacCormack algorithm. The total enthalpy, H, in the energy equation has to be evaluated according to the formula in Eq. (2.20). The finite-difference representation of the species equations results in a block-diagonal system of algebraic equations and is inverted pointwise by an L-U decomposition procedure.

Once all the conservative variables are obtained at a time step, the primitive variables have to be deciphered from them. Some difficulties arise in deciphering the temperature, T. The solution of the energy equation gives the quantity $(\rho H - p)$ of the mixture. This study assumes that the thermodynamic property, $\bar{C}_p$, of the mixture can be lagged one time step without causing any significant error. With the above assumption the term $(\rho H - p)$ can be written as

$$\rho H - p = \rho \bar{C}_p^{*} T + \frac{1}{2} \rho (u^2 + v^2) - \rho \bar{R} T \qquad (4.1)$$

where the starred quantity is to be evaluated at the old time level. The term $\bar{C}_p^{*}$ is defined as (see Eq. (2.20))

$$\bar{C}_p^{*} = \sum_{i=1}^{5} [f_i (0.5\, a_i\, T^{*} + b_i)]. \qquad (4.2)$$

By using Eq. (4.2) in Eq. (4.1) the temperature of the new time level can be obtained directly without having to solve a second-order algebraic equation

in T. Finally, the pressure, p, is calculated from the ideal gas equation of state using the mixture gas constant $\bar{R}$.

5. RESULTS AND DISCUSSION

The non-reacting computer code of Refs. 14-15 has been modified to incorporate the chemistry package as described in the previous sections. The code is written specifically for the VPS-32 vector processing computer at the NASA Langley Research Center. The program was used to solve two model problems of supersonic combustion of premixed hydrogen-air systems.

The geometry as well as the inflow conditions of the first test case are shown in Fig. 1. The equivalence ratio (ϕ) for this case is 0.2. The inflow gas is assumed to be a perfect mixture of hydrogen and air. A grid of 31x31 is used in this test case; it is shown in Fig. 2. The velocity vectors of the solution are illustrated in Fig. 3. The vectors are well behaved everywhere with indication of boundary layers developed close to the solid walls. Note that, in addition to the assumption of laminar flow, the grid use for this analysis is too coarse to resolve the detail of the boundary layers. The main purpose of this test case was, however, to check for coding errors and not to capture all the details of the flow. The pressure contours are indicated in Fig. 4. The big bubble at the inflow boundary is a consequence of initial formation of the OH species which is endothermic. The shock wave emanating from the compression corner is clearly seen in the figure. Figs. 5, 6 and 7 show the concentration contours of OH, H_2 and O_2, respectively. These figures exhibit one common feature in that they all show a concentration shock at the inflow boundary. The formation of these shocks are physically reasonable because the OH species was produced at a very fast rate. In fact, it is the fast production of the OH species that gives rise to the stiffness of this problem in the first place. The H_2 and O_2 shocks were formed simply because OH was produced at the expense of H_2 and O_2. The concentration contours of H_2O in Fig. 8, however, does

not indicate any concentration shock at the inflow boundary; instead H_2O is produced in a continuous fashion. This is compatible with the physics of the current chemistry model in that H_2O production is much slower than that of OH. Figs. 9 and 10 show the mass-fraction distributions of various species at y station 15 and 5, respectively. The step changes of the concentration of OH, H_2 and O_2 are clearly seen at the inflow boundary whereas continuous increase in the level of H_2O is observed. The extent of reaction in Fig. 10 is higher than that of Fig. 9 due to the fact that the temperature level of Fig. 10 is higher than that of Fig. 9 because the flow passed through the shock wave.

For the second test case, the geometery and inflow conditions (Fig. 11) are mostly the same as the first test case except M_∞ is changed to 4 and ϕ changed to 1.0. The increase in the value of ϕ should make this test case a lot more severe than the previous one. In addition, the flow is assumed turbulent and the grid is a 31x51 system (Fig. 12) with proper stretching near solid walls in order to resolve the boundary-layer's details. Moreover, a reaction switch is incorporated into the code. The switch turns the reaction on only when the temperature is greater than 1000K. The threshold temperature of 1000K is a realistic one for the present H_2-air system. Since the inflow temperature is 900 K, there should be no reaction until a shock wave raises the temperature of the mixture to above 1000K. Figs. 13 and 14 show the concentration contours of OH and H_2O, respectively. These two figures indicate, as expected, no reaction in the free stream; the reaction occurs only after the shock or inside the boundary layers where the temperature is above 1000K. Fig. 13 indicates OH-concentration shock coinciding with the pressure shock whereas a more-or-less continuous production of H_2O is observed in Fig. 14. Fig. 15 shows

the concentration profiles of various species along the 15th y station. All distributions in the figure are as expected. The OH concentration rises much faster than that of H_2O whereas O_2 and H_2 concentrations reduce continuously. About 80 percent of H_2 is consumed within the resident time of about 10×10^{-6} second. The plot also indicates that this short resident time is not enough for OH to recombine with H_2 to form an appreciable amount of the final product, H_2O. Finally, the concentration distributions at the second y station (inside the hot boundary layer) is illustrated in Fig. 16. The reaction starts right at the leading edge and shows a small jump near the shock wave.

6. CONCLUSIONS

The chemistry package added to the non-reacting Navier-Stokes code seems to predict the correct pnysics of this particular H_2-air combustion system. The present code assumes a premixed mixture of H_2 and air at the inflow boundary. For a stratified H_2-air system, a minor modification to the code must be made. It is observed that most of the computer time is used to invert the block-diagonal matrix of the species equations. A more efficient algorithm to invert these blocks either directly or indirectly is highly desirable, especially the one that is suitable for vector processing.

Current effort is being directed toward solving a realistic supersonic H_2-air combustion system. Instead of a premixed assumption, the fuel (H_2) is injected as a stream into the mainflow. Results of the current investigation will be reported at a later date.

REFERENCES

1. Anderson, G. Y.: Hypersonic Propulsion. Paper No. XV, NASA SP-381, 1975.

2. Jones, R. A. and Huber, P. W. Toward Scramjet Aircraft. Astronautics and Aeronautics, Vol. 16, No. 2, 1978, pp. 38-49.

3. Beach, H. L., Jr.: Hypersonic Propulsion. Paper No. XII, NASA CP-2092, 1979.

4. Kumar, Ajay: Numerical Analysis of the Scramjet Inlet Flow Field Using Two-Dimensional Navier-Stokes Equations. AIAA Paper 81-185, 1981.

5. Kumar, Ajay and Tiwari, S. N.: Analysis of the Scramjet Inlet Flow Field Using Two-Dimensional Navier-Stokes Equations. NASA CR 3562, June 1982.

6. Kumar, A.: Numerical Analysis of a Scramjet Inlet Flow Field Using the Three-Dimensional Navier-Stokes Equation. Presented at the 1983 JANAF Propulsion Meeting, February 1983.

7. Drummond, J. P. and Weidner, E. H.: Numerical Study of a Scramjet Engine Flo Field. AIAA Journal, Vol. 20, No. 9, September 1982.

8. Rogers, R. C. and Schexnayder, C. J., Jr.: Chemical Kinetic Analysis of Hydrogen-Air Ignition and Reaction Time. NASA TP 1856, 1981.

9. Rogers, R. C. and Chinitz, W.: Using a Global Hydrogen-Air Combustion Model in Turbulent Reacting Flow Calculations. AIAA Journal, Vol. 21, No. 4, April 1983.

10. Stalnaker, J. F., Robinson, M. A., Spradley, L. W., Kurzius, S. C. and Thoenes, J.: Development of the General Interpolants Method for the Cyber 200 Series of Computers. Report TR D867354, Lockheed-Huntsville Research and Engineering Center, Huntsville, AL, October 1983.

11. Smoot, L. D., Hecker, W. C. and Williams, G. A.: Prediction of Propagating Methane-Air Flames. Combustion and Flame, Vol. 26, 1976.

12. Drummond, J. P., Hussaini, M. Y. and Zang, T.: Spectral Methods for Modeling Supersonic Chemically Reacting Flow Fields, AIAA Paper 85-0302, January 1985.

13. Bussing, T. R. A. and Murman, E. M.: A Finite Volume Method for Calculation of Compressed Chemically Reacting Flows. AIAA Paper No. 85-0331, January 1985.

14. Kumar, A.: Some Observations on a New Numerical Method for Solving the Navier-Stokes Equations. NASA TP-1940, November 1981.

15. Kumar, A.: User's Guide for NASCRIN-A Vectorized Code for Calculating Two-Dimensional Supersonic Internal Flow Fields. NASA TM 85708, February 1984.

16. Baldwin, B. S. and Lomax, H.: Thin Layer Approximation and Algebraic Model for Separated Turbulent Flows. AIAA Paper No. 78-257, January 1978.

17. Kays, W. M. and Crawford, M. E.: Convective Heat and Mass Transfer. McGraw-Hill, New York, 1980.

18. McBride, B. J., Heimel, S., Ehlens, J. G., and Gordon, S.: Thermodynamic Properties to 6000°K for 210 Substances Involving the First 18 Elements. NASA SP-3001, 1963.

19. Drummond, J. P.: Private communication.

20. MacCormack, R. W.: The Effect of Viscosity in Hypevelocity Impact Cratering. AIAA Paper No. 69-354, May 1969.

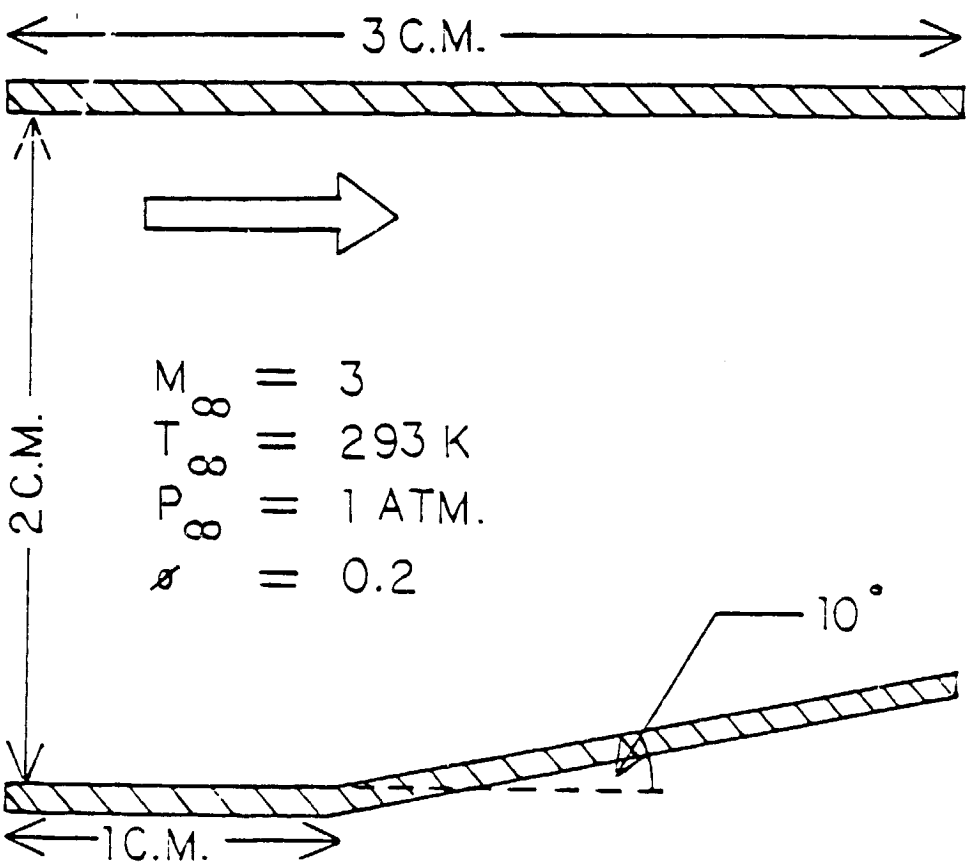

Figure 1. Geometry and inflow conditions of test case no. 1.

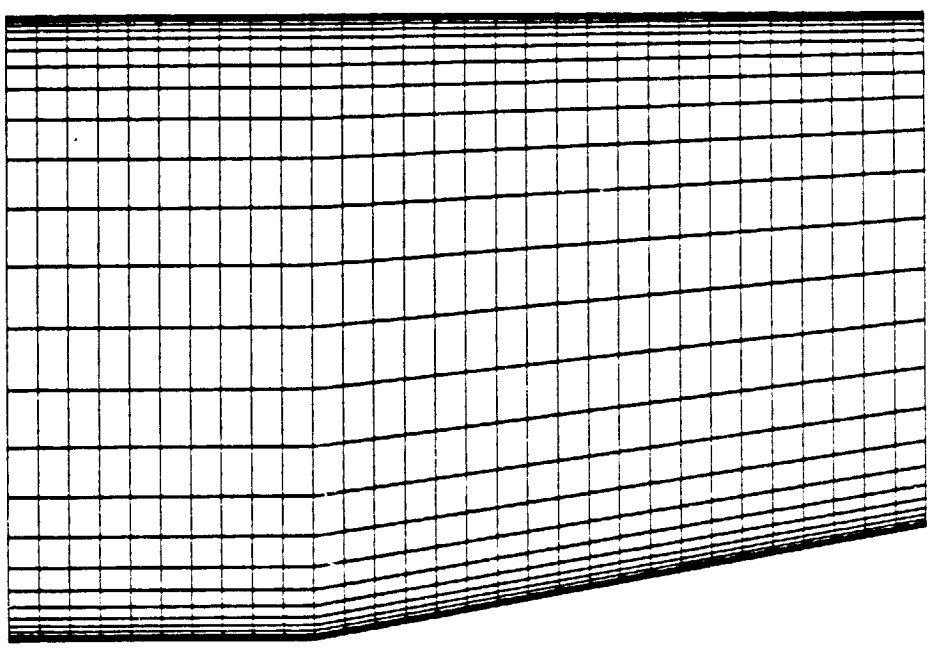

Figure 2. Grid system of test case no. 1.

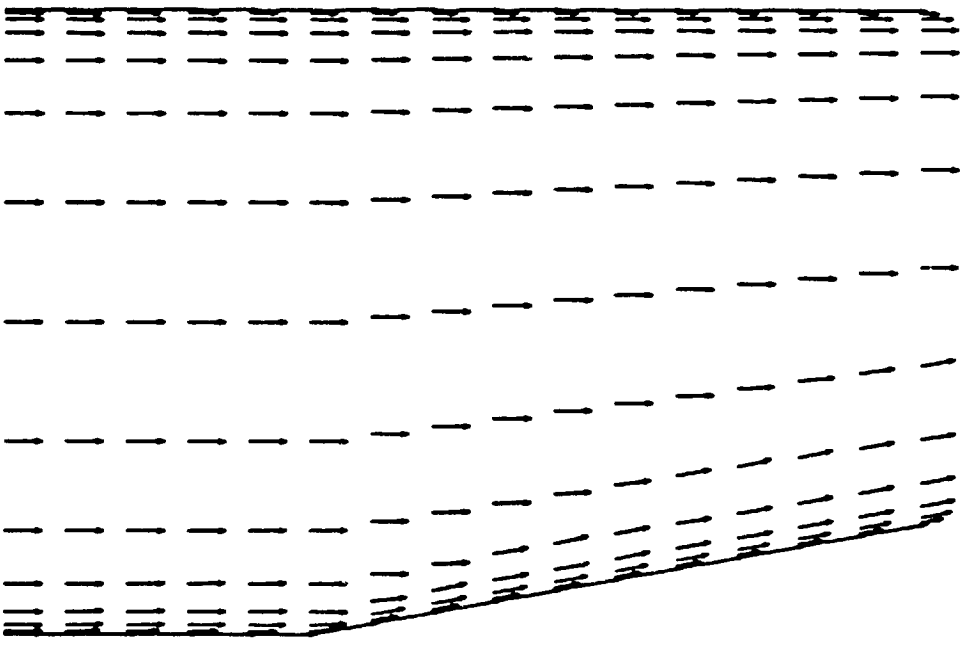

Figure 3. Velocity vectors of case 1.

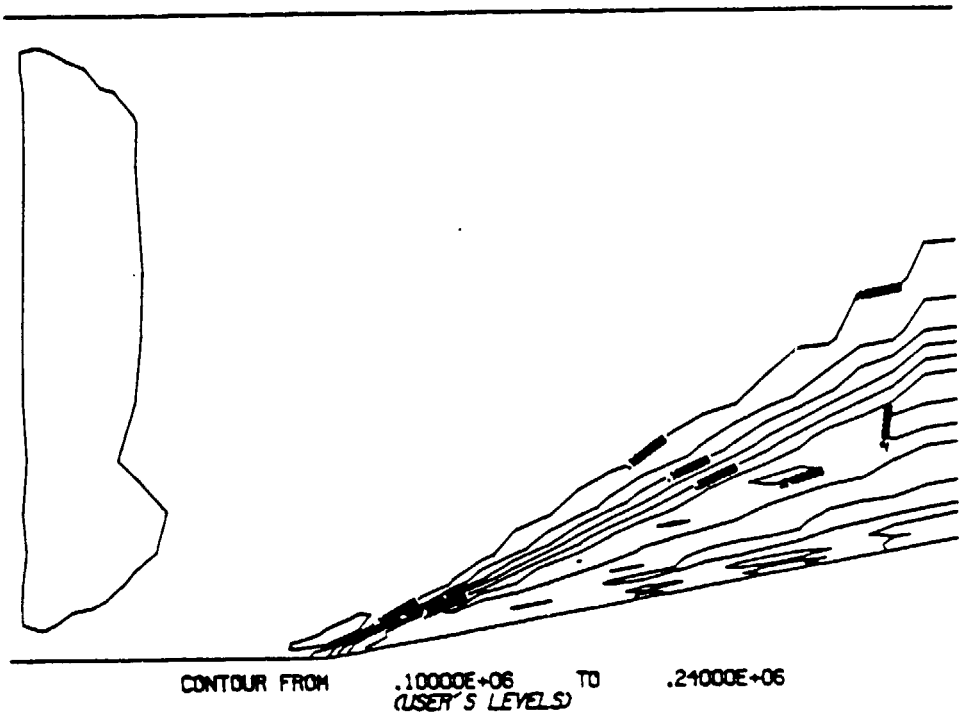

Figure 4. Pressure contours of case 1.

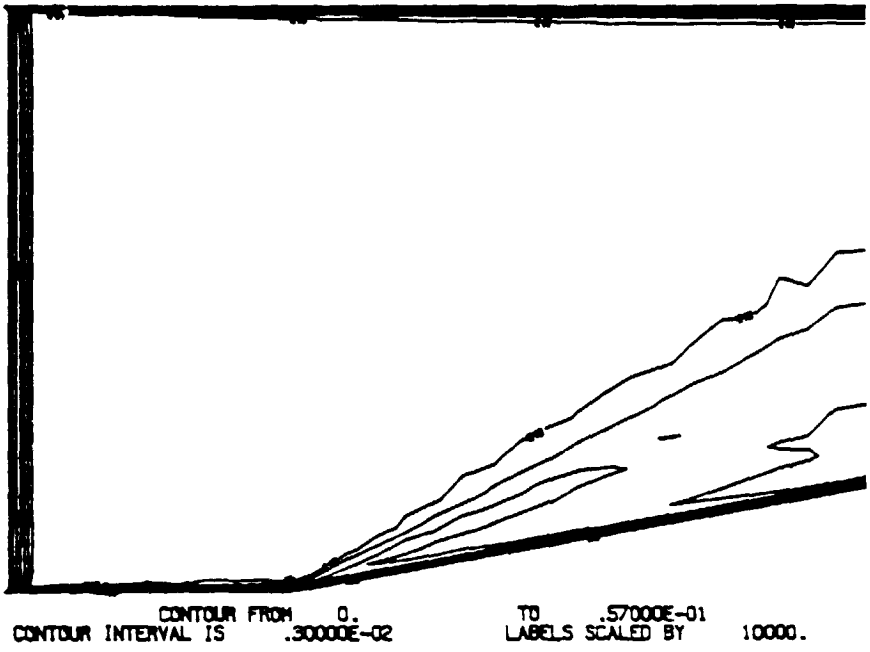

Figure 5. OH-concentration contours of case 1.

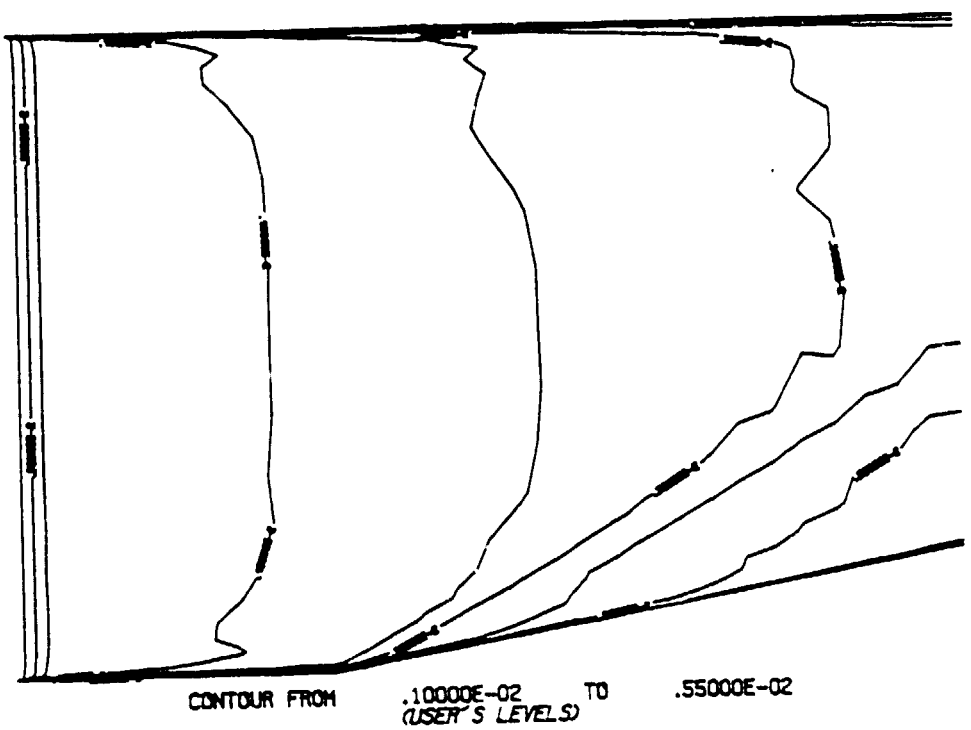

Figure 6. H_2-concentration contours of case 1.

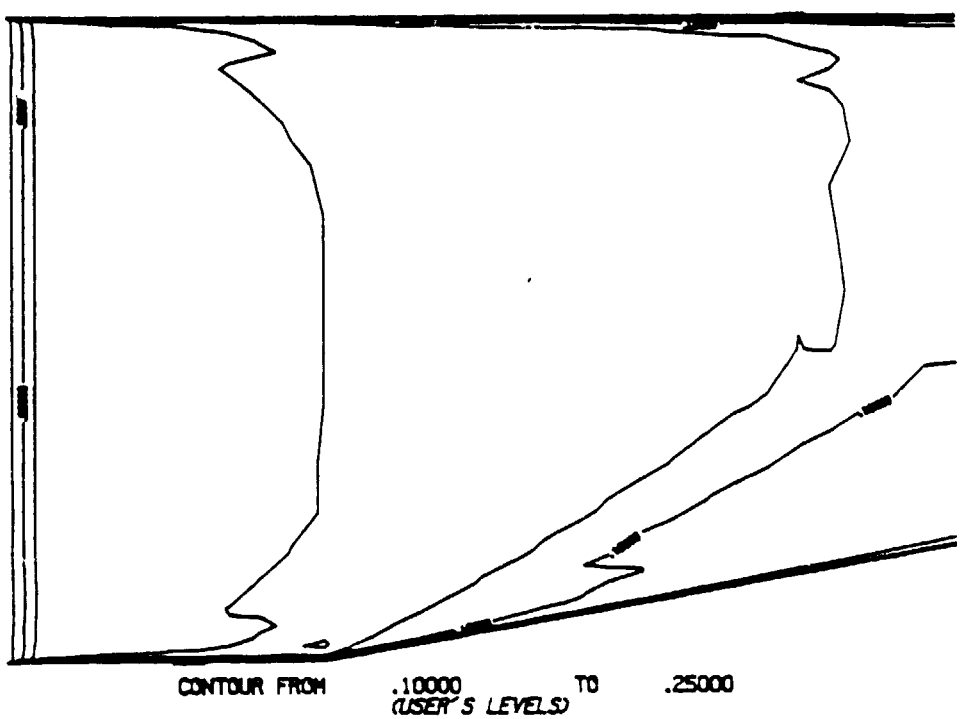

Figure 7. O_2-concentration contours of case 1.

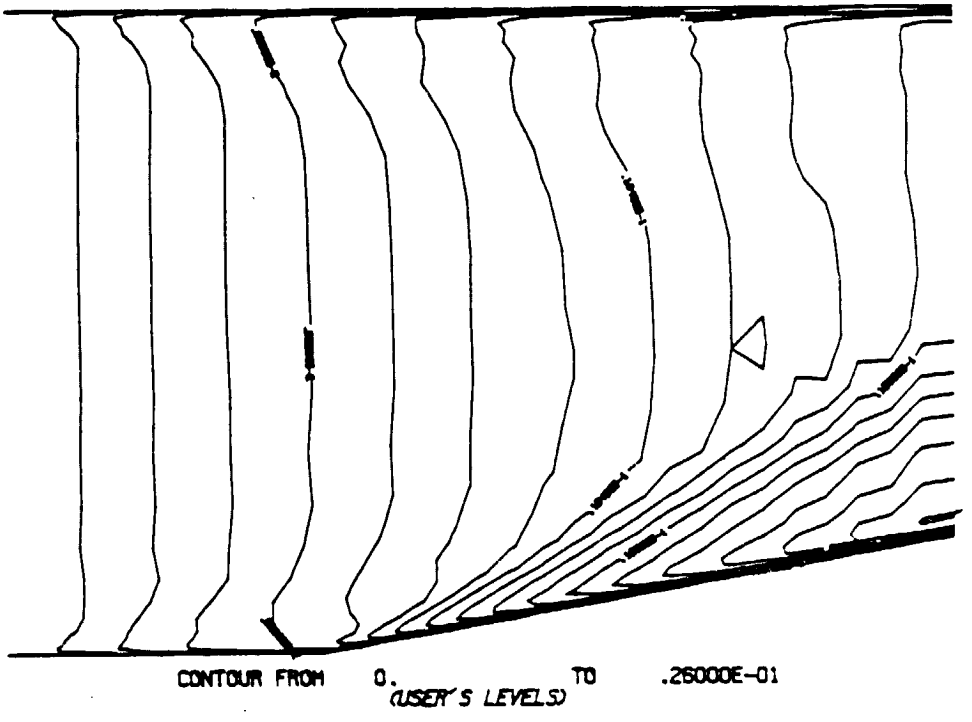

Figure 8. H_2O-concentration contours of case 1.

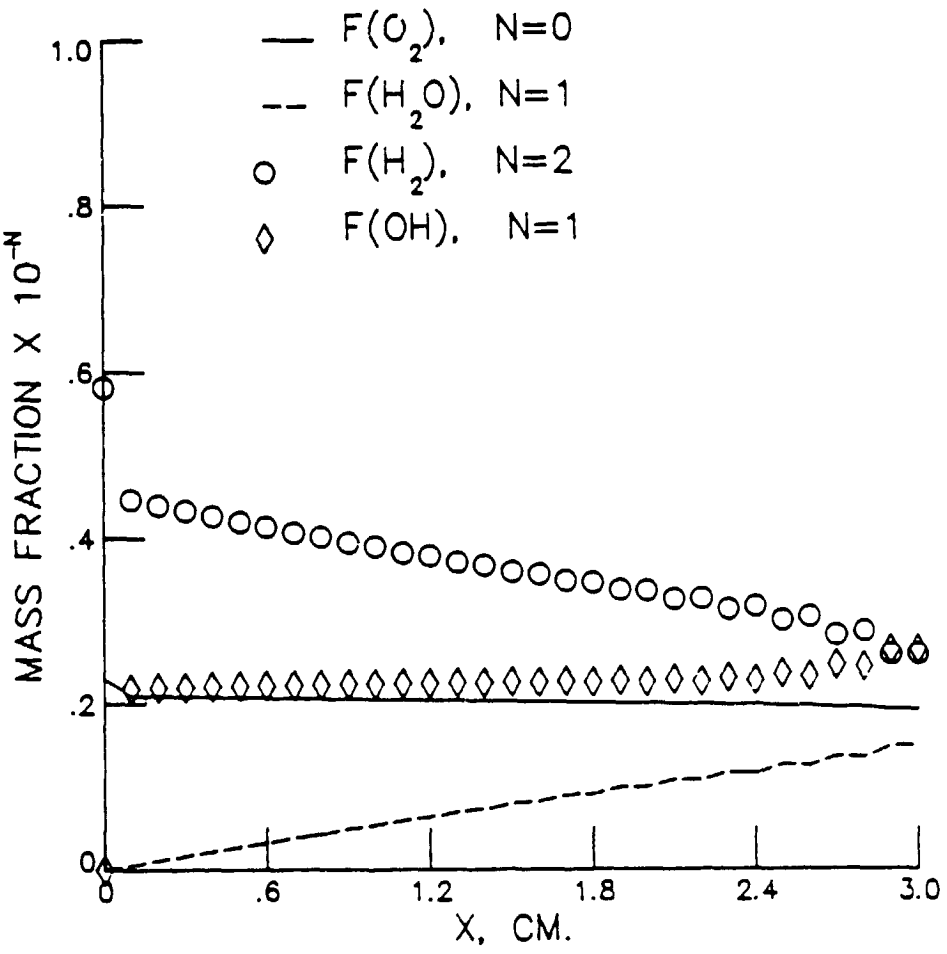

Figure 9. Mass-fraction distributions at y-station no. 15.

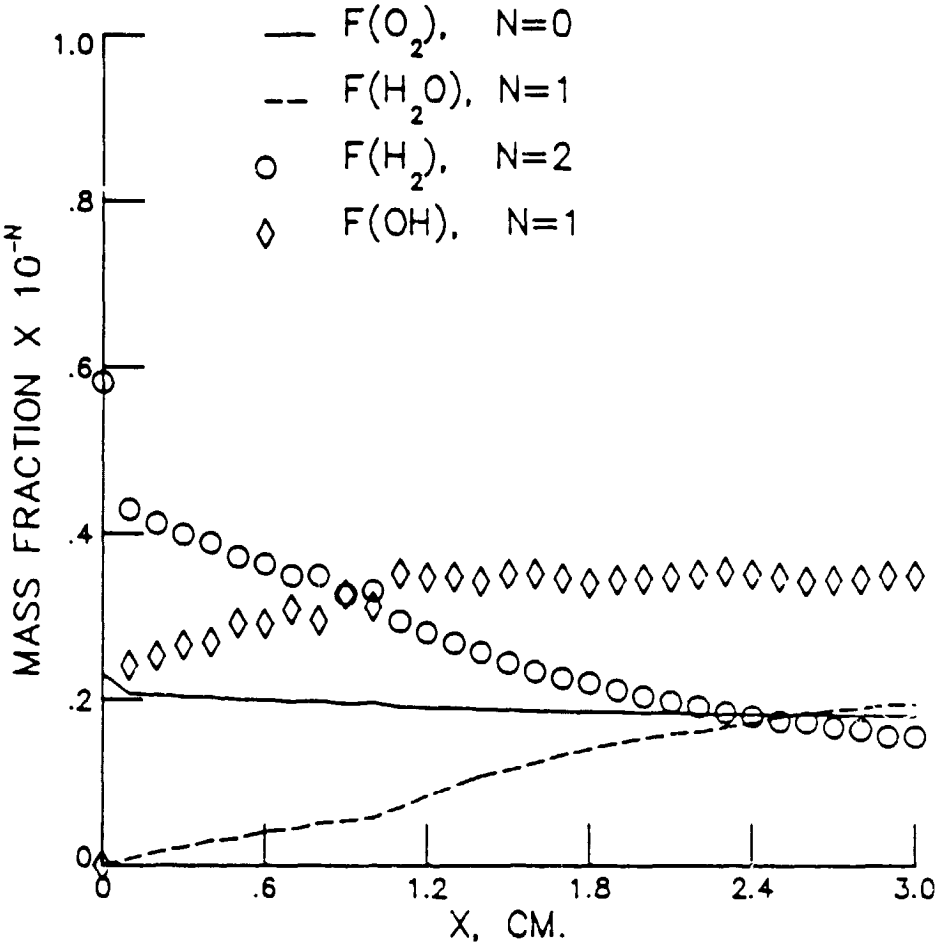

Figure 10. Mass-fraction distributions at y-station no. 15.

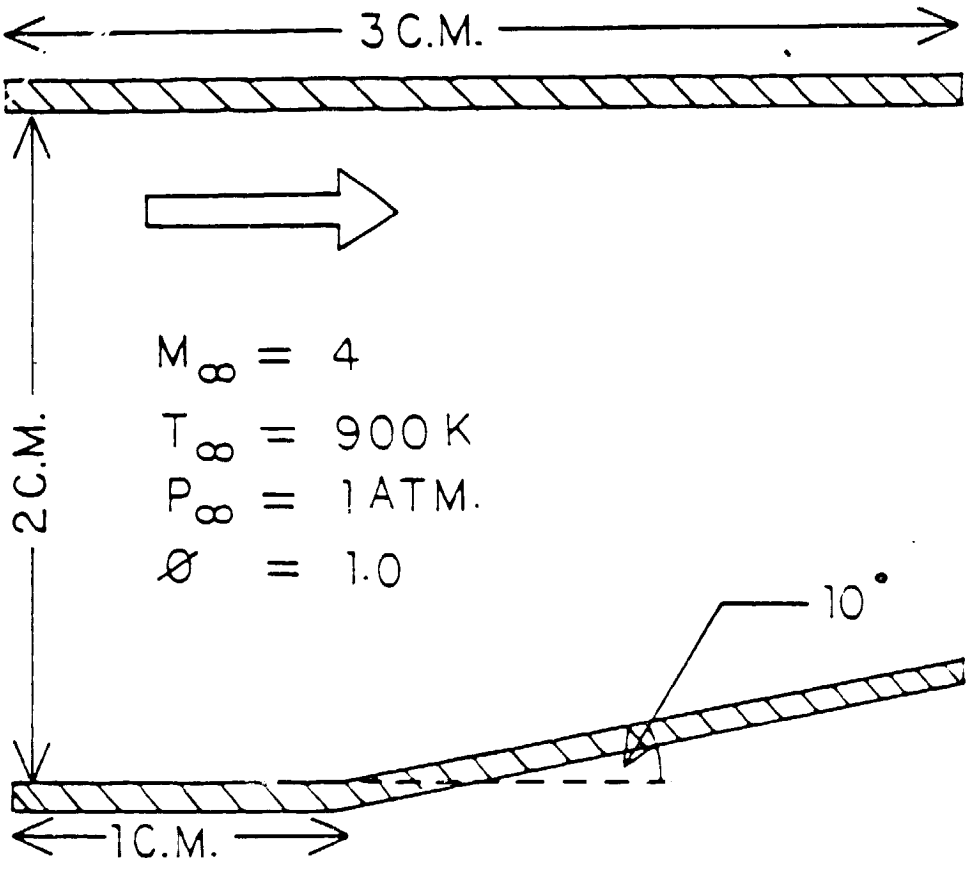

Figure 11. Geometry and inflow conditions of test case no. 2.

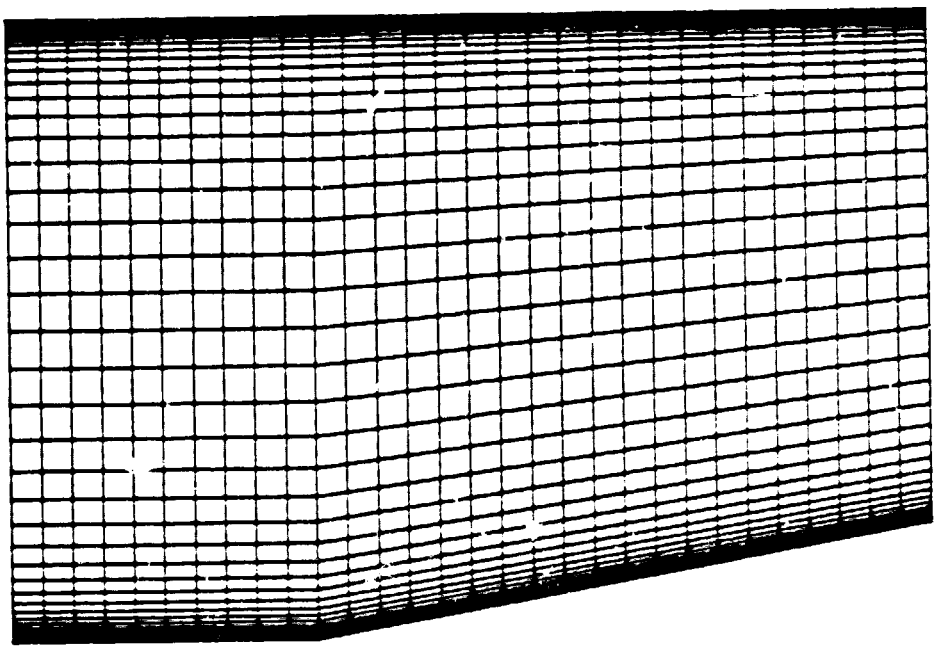

Figure 12. 31x51 grid system of case 2.

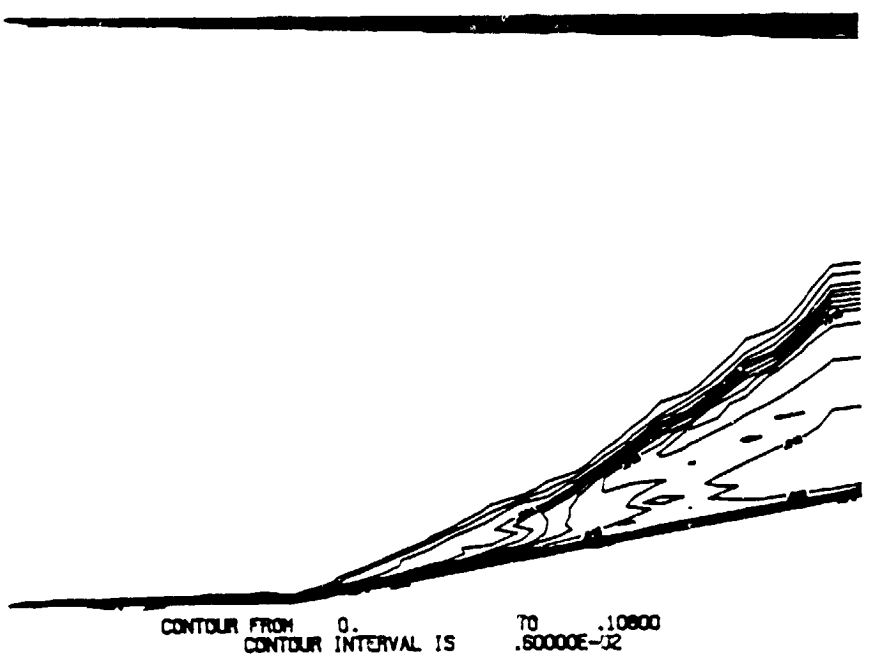

Figure 13. OH-concentration contours of case 2.

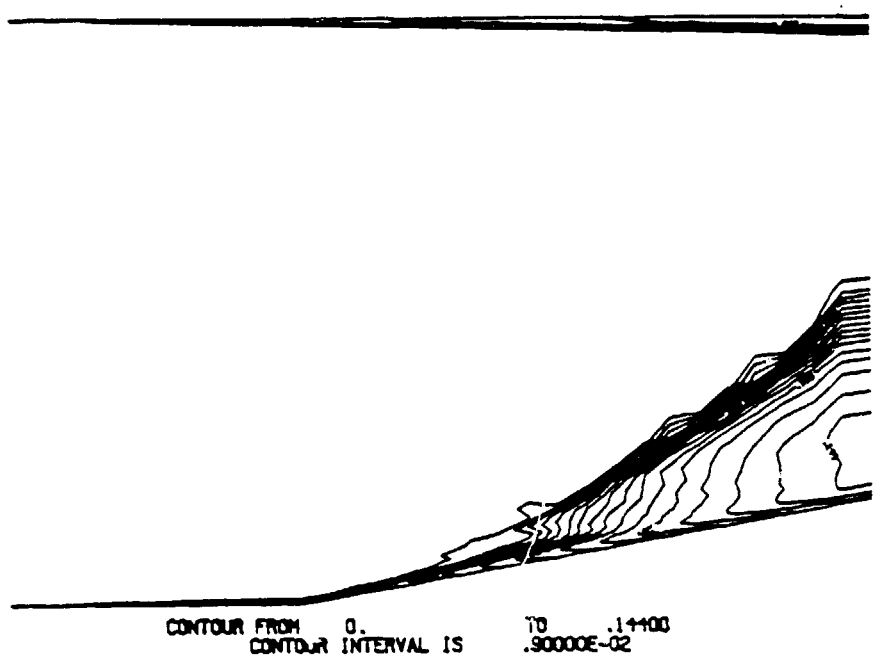

Figure 14. H_2O-concentration contours of case 2.

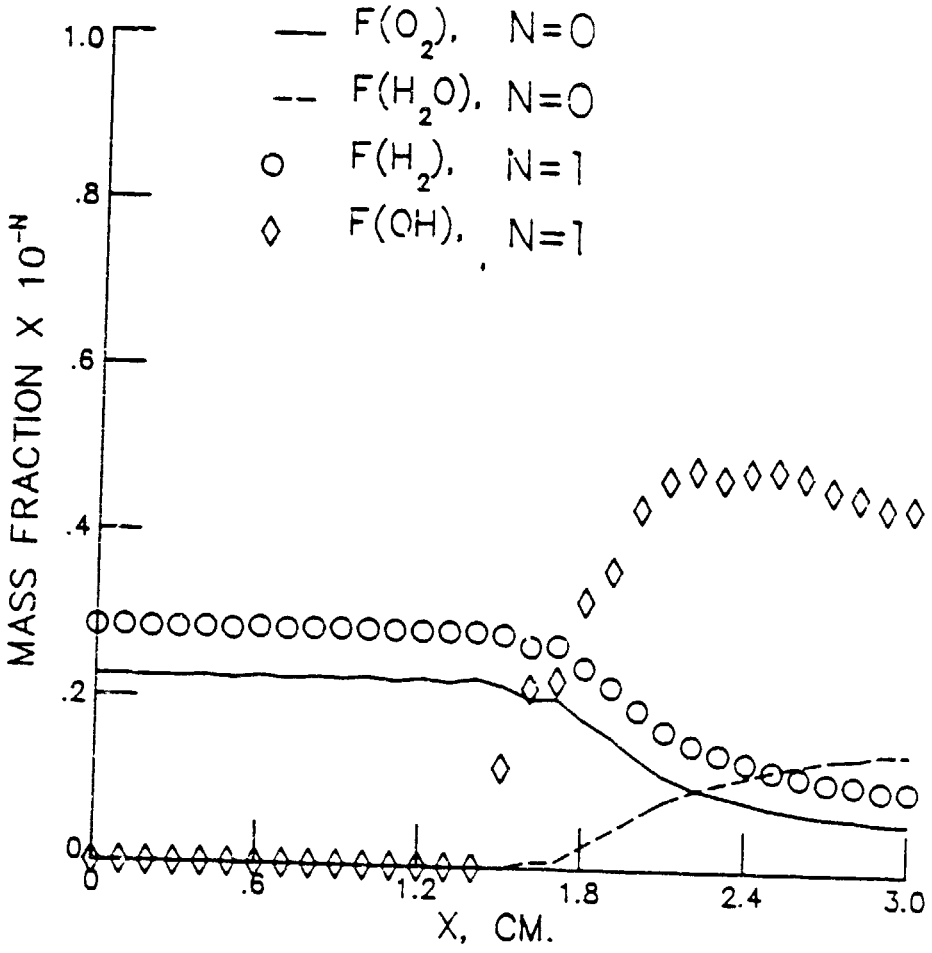

Figure 15. Mass-fraction distributions at y-station no. 15.

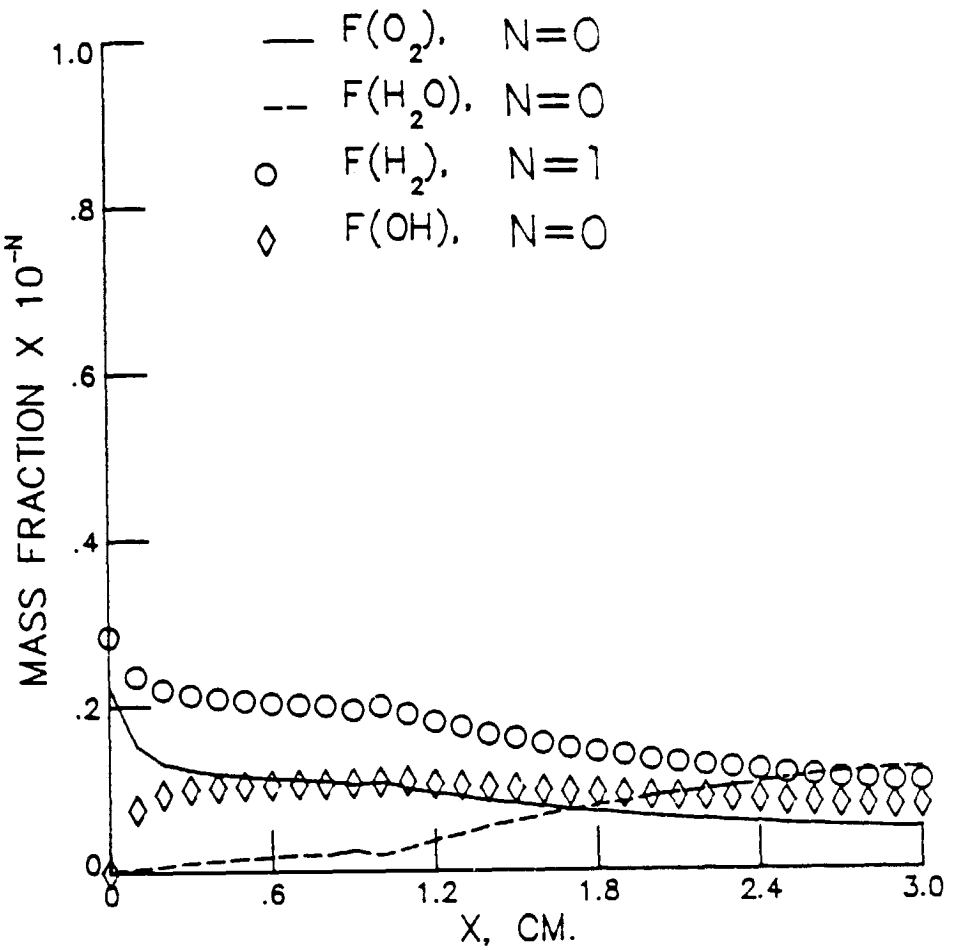

Figure 16. Mass-fraction distributions at y-station no. 15.